Research article

NAR2.1/NRT2.1 functional interaction with NO3- and H+ fluxes in high-affinity nitrate transport in maize root regions

Antonio Lupini [a], Francesco Mercati [b], Fabrizio Araniti [a], Anthony J. Miller [c], Francesco Sunseri [a], Maria Rosa Abenavoli [a]

a Dipartimento di Agraria, Universita Mediterranea di Reggio Calabria, Salita Melissari, I-89124, Reggio Calabria, Italy

b Institute of Biosciences and Bioresources (IBBR), National Research Council of Italy (CNR), Corso Calatafimi, 414, I-90129, Palermo, Italy

c John Innes Centre, Norwich Research Park, Norwich, NR4 7UH, UK

Abstract

Spatial and temporal fluctuations in nitrate (NO_3^-) availability are very common in agricultural soils. Therefore, understanding the molecular and physiological mechanisms involved in regulating NO_3^- uptake in regions along the primary root is important for improving the NO-3 uptake efficiency (NUpE) in crops. Different regions of maize primary root, named R1, R2 and R3, NO-3 starved for 3 days, were exposed to 50 μM NO-3. Electrophysiological measurements (membrane potential and H+ and NO_3^- fluxes) and NPF6.3, NRT2.1, NAR2.1, MHA1, MHA3 and MHA4 gene expression analyses were carried out. The results confirmed variable spatial and temporal patterns in both NO_3^- and H+ fluxes and gene expression along the primary maize root. A significant correlation (P=0.0023) between nitrate influx and gene transcript levels was observed only when NAR2.1 and NRT2.1 co-expression were considered together, showing for the first time the NRT2.1/NAR2.1 functional interaction in nitrate uptake along the root axis. Taken together these results suggest differing roles among the primary root regions, in which the apical part seem to be involved to sensing and signaling in contrast with the basal root which appears to be implicate in nitrate acquisition.

Keywords: Ion-selective microelectrode, Maize root regions, MHA gene family, *NAR2.1*, *NPF6.3*, *NRT2.1*

1. Introduction

Nitrogen, as an essential component of proteins, nucleic acids, chlorophyll and many secondary metabolites, is one of the major limiting factors for plant growth and productivity. Therefore, a huge amount (about 100 million tons) of N fertilizer is applied to improve crops yield annually (FAO, 2006), representing the major cost for agricultural systems (Masclaux-Daubresse et al., 2010). Among N sources, nitrate (NO^-_3) is the primary inorganic N mobile form available in agriculture soils and its concentration varied widely (typically range between 0.5 and 10 mM) in the soil solution (Miller et al., 2007). To cope with its high spatial and temporal fluctuation (Krouk et al., 2010), plants have evolved highly flexible and dynamic transport systems to acquire this anion. In particular, three transport systems coexist in plants to take up NO^-_3 from the soil solution: a constitutive (cHATS) and an inducible (iHATS) high-affinity transport systems (up to 500 μM NO^-_3), and a low-affinity transport system (LATS) (higher than 500 mM NO^-_3) (for review, see Crawford and Glass, 1998;

Glass, 2009). Nitrate transporters belong to five protein families, NPF, NRT2, CLC, ALMT, SLAC1 (Barbier-Brygoo et al., 2011; Leran et al., 2014) have been identified, but only NPF and NRT2 families were significantly involved in nitrate root uptake (Nacry et al., 2013). Among the seven genes of NRT2 family (Okamoto et al., 2003), the major contributor of the total HATS activity is NRT2.1 (Li et al., 2007), whereas LATS is encoded by NPF family members. An exception is NPF6.3 (NRT1.1 or CHL1), which is a dual-affinity nitrate transporter (Ho et al., 2009). Moreover, recently using maize plants high nitrate use efficiency was identified as being consistent with uptake at low nitrate supply (El-kereamy et al., 2011; Garnet et al., 2013; Zamboni et al., 2014). Among different genes belonging to the NRT2 family, NRT2.1 in interaction with NAR2 protein (Orsel et al., 2006), plays a major role in nitrate uptake in iHATS system in the whole root system of many plants and along the maize primary root (Tong et al., 2005; Okamoto et al., 2006; Wirth et al., 2007; Sorgona et al., 2011; Yan et al., 2011). Plasma membrane (PM) H+-ATPase ensured the energy required for NO^-_3 acquisition, showing a similar time-course pattern of NO^-_3 uptake in wood and crop species (Miller and Smith, 1996; Santi et al., 1995; Sorgona et al., 2010, 2011). In maize, MHA3 and MHA4 genes member of the PM $H_þ$-ATPase subfamily II appeared to be closely involved in nitrate uptake (Santi et al., 2003; Sorgona et al., 2011). In the past few decades, spatial and temporal variability in NO^-_3 uptake along the root axis in herbaceous (Colmer and Bloom,1998; Henriksen et al.,1992; Sorgona et al., 2011; Taylor and Bloom, 1998) and woody plants (Hawkins et al., 2008; Luo et al., 2013; Sorgona et al., 2010), has been reported, sometimes with contrasting results. Recently, Sorgona et al. (2011) confirmed the spatial and temporal heterogeneity of the NO^-_3 uptake patterns along maize root axis, underlying the important role of the apical root region in NO^-_3 acquisition. Moreover, the authors highlighted a strong temporal correlation between NRT2.1 and net nitrate uptake rate (NNUR) activity, which failed at spatial level, speculating on the involvement of NAR2 protein as essential partner for iHATS function also along maize primary root axis (Sorgona et al., 2011). In order to validate this hypothesis, in the present study, the spatial and temporal gene expression patterns of NAR2.1 together with NRT2.1, NPF6.3 (for nitrate transport), MHA3 and MHA4 (for PM H+-ATPase) were evaluated along maize primary root. In addition, NO^-_3 and H^+ fluxes and the thermodynamic or free energy gradient for nitrate transport across the plasma membrane were also estimated, to better understand their different role in NO^-_3 uptake within the apical root region in response to this anion.

2. Materials and Methods

2.1. Plant material and growth conditions

Maize (Zea mays L., hybrid cv. Cecilia, Pioneer Hi-bred Italia Spa) seeds, surface sterilized for 20 min in 10% (v/v) sodium hypochlorite solution and rinsed with deionized water, were germinated in darkness at 24 C in a plastic container filled with 0.5 mM CaSO4 for 72 h. Uniform size seedlings were transferred into a growing unit containing 4.3 L of aerated one-quarter-strength Hoagland solution without N, and placed in a growth chamber at 24 C with a 14 h photoperiod, a photon flux density of 350 mmol m^{-2} s^{-1} and 70% RH for 4 d. The nutrient solution pH was adjusted to 6.0 with 0.1 M KOH. To study the mechanism of regulation of nitrate uptake these uninduced plants (7-d old) were exposed to 50 μM KNO_3 and at 0, 4 and 24 h before the experiments were performed. Three primary root regions were defined according to the distance from the root apex: 0-20, 21-40, 41-100 mm e hereafter named R1, R2 and R3, respectively.

2.2. Membrane potential measurements

The membrane electrical potential of the outermost layer of cells was measured using standard glass microelectrode techniques in R1, R2 and R3 regions after 0, 4 and 24 h of exposure to 50 mM NO_3^-. Single-barreled microelectrodes were prepared using filamented borosilicate glass as previously described (Lupini et al., 2010). The microelectrode was backfilled with 200 mM KCl solution using a 70 mm long Microfil needle (World Precision Instruments Inc., Stevenage, UK). The whole maize primary root was placed in a Plexiglas chamber for the electrode impalement with a basic buffer solution containing 0.2 mM KCl, 0.5 mM CaCl2,1 mM MES-KOH (pH 6) at room temperature (24e26 C). Impalements with microelectrodes were always carried out in mature epidermal cells, measuring the voltage difference (mV) between the inside of the cell and the external bathing solution. The values from 80 to 140 mV were considered to define a successful cell microelectrode impalement and measurement. The initial impalement of the epidermal cell could be visually confirmed and by the accompanying jump in the recorded voltage after which it was not possible to see the exact location of the tip. Before each measurement, a time interval (5 min) of stable cell electrical membrane potential was recorded (data not shown).

2.3. NO-3 and H^+ fluxes measurements

Using a non-invasive microelectrode ion flux system, $NO_3^-$and H+ fluxes in R1, R2 and R3 regions (at 10, 30 and 50 mm from root tip, respectively), were concurrently performed after 0, 4 and 24 h of exposure to 50 μM NO_3^-, at room temperature (24-26° C). Briefly, borosilicate glass capillaries were pulled and dried in oven at 220 C overnight to dehydrate, and rendered hydrophobic by addition of Silanization solution I (Sigma-Aldrich Chemicals Co., MO, USA). Cooled microelectrodes were backfilled with 500 mM KNO_3 plus 100 mM KCl, and 15 mM NaCl plus 40 mM KH2PO4 (adjusted to pH 6.0 using 0.1 M NaOH) for NO-3 and Hþ, respectively. Electrode tips were filled with commercial H+ or NO_3^- ionophore (Fluka n. 95297 and 72549, respectively). A plastic tube containing 1 M KCl in 2% (w/v) agar was used as reference electrode. Before using, electrodes were calibrated against a range of standards (pNO_3^- from 1 to 5 and pH from 5 to 7.2). Electrodes with responses less to 50 mV/pIon were discarded. Maize seedlings exposed to NO_3^- were suddenly equilibrated in a solution containing a basic unbuffer solution plus 50 μM KNO3 for 10 min. The roots were placed in a Plexiglas chamber containing 4 ml of same solution and each electrode tip (NO_3^- or H+) was positioned at 10 mm above root surface and attached to a computer-controlled micromanipulator (PatchMan NP2, Eppendorf AG, Hamburg, Germany) which gently moved between two positions (with a distance of 40 mm) at a frequency of 0.1 Hz. The concentration of each ion was calculated and the flux was estimated as reported by Newman (2001). Data analysis was performed using DataTrax2 v. 2.079 software (World Precision Instruments Inc., USA).

2.4. Gene expression analysis

2.4.1. RNA extraction

Total RNA from R1, R2 and R3 root regions of maize seedlings (7 days old) was extracted from 100 mg of fresh tissue after 0, 4 and 24 h of exposure to 50 μM NO_3^-. RNA was isolated using RNeasy Plant Mini Kit (Qiagen, Milano, Italy), following the manufacturer's instructions. The RNA quality and quantification were assayed by NanoDrop 2000 (Thermo Scientific).

2.4.2. RT-PCR

Qualitative Reverse Transcript-PCR (RT-PCR) experiments starting from 100 ng of total RNA in 25 µl reaction (QIAGEN OneStep RT-PCR kit) for each treatment (root regions and times) were used to detect NAR2.1, NPF6.3, NRT2.1, MHA3 and MHA4 genes. Specific primers for each gene were designed on the basis of sequences available in NCBI database. Ubiquitin (Bio-Fab research s.r.l., Roma, Italy) was used as housekeeping (Table S1). A set of different numbers of cycles ranging between 25 and 35 was tested to choose those corresponding to the exponential phase for each gene. The PCR reactions were performed under the following condition: 30 cycle of 30 s at 94 C (denaturation), 45 s at 64 C (annealing) and 60 s at 72 C (extension); a 30 min reverse transcription at 55 C; a 15 min hot start at 95 C at the beginning of the reactions and finally a 10 min extension at 72 C were performed. The PCR products were verified in agarose gel (1.5% w/v) using 123 bp DNA ladder (Invitrogen) as molecular standard. All PCR experiments were repeated five times to confirm the repeatability of the banding patterns.

2.4.3. qPCR

First-strand cDNA was synthesized from 1 mg of total RNA after DNase treatment, using QuantiTect Reverse Transcription Kit (Qiagen, Milano, Italy), following the protocol provided by the manufacturer. Real-Time quantitative PCR (qPCR) was performed using the SYBR® Green RT-PCR master mix kit (Applied Biosystem, Branchburg, NJ, USA) adding 1 ml of cDNA, 0.2 mM of the specific primer and 12.5 ml of 2X SYBR Green PCR Master Mix, in 25 ml total volume as suggested by manufacturer's protocol. Four replicates for each treatment were performed. The conditions of amplifications were performed as previously described by Sorgona et al. (2011) . According to the quantification method (Livak and Schmittgen, 2001), specific primers were designed to amplify target fragments (Table S2). The qPCR results were analyzed by the 2DDCT comparative method as previously described in User Bulletin No 2 (Applied Biosystems) and reported in Livak and Schmittgen (2001).

3. Statistical analysis

A completely randomized experimental design was adopted, with five replicates. All data were checked for normality (Kolmogorov-Smirnov test) and tested for homogeneity (Leven median test). The effects of NO_3^- on membrane potential of R1, R2 and R3 regions of primary maize root were tested by one-way ANOVA within time of exposure. Nitrate and H+ fluxes were tested by twoway ANOVA, taking into account the R1, R2 and R3 regions and the time of exposure (0, 4 and 24 h) as factors. Further, Tukey's HSD test (p = 0.05) was applied to compare the mean values. Thermodynamics or free energy gradient for nitrate transport across plasma membrane was estimated by the equation proposed by Miller and Smith (1996):

$$\Delta G'/F = 59\{n(pH_o - pH_c) + (p[NO_3]_o - p[NO_3]_c)\} + (n-1)\Delta\Psi$$

where n is the stoichiometry ($H:NO_3^-$, 2:1) of proton to nitrate ions for the symport, DJ is the trans-plasma membrane potential difference and subscripts o and c denote the external solution and cytosol, respectively. The pHc and $p[NO_3]c$ values were used according to Miller and Smith (1996). Finally, Pearson correlation ($P < 0.05$) between gene transcript abundances and ion fluxes was estimated. Statistical analysis was performed using Systat v. 8.0 software package (SPSS Inc.).

4. Results

4.1. Membrane potential and ion flux measurements

In preliminary experiments, the flux measurements were carried out at different points within each region (data not shown) and the single area identified, was taken as being representative of the entire region. Root cell membrane potentials in R1, R2 and R3 regions, before (0 h) and after (4 and 24 h) NO_3^- exposure were recorded. At 0 h, after the stabilization of Em (5 min) in a basic buffer solution without NO_3^-, the Em values were significantly different among the three root regions (Fig. 1). In particular, R1 showed a higher membrane potential (more negative, 107.5 ± 2.0 mV) compared to R2 and R3, which showed no significant difference between them (83.3 ± 5.5, and 84.8 ± 4.3, respectively) (Fig. 1). A similar pattern was also observed after 4 h of NO_3^- exposure, where a high membrane hyperpolarization was recorded in all root regions, with a significant higher Em value in R1(-121 mV) compared to R2 (99 mV) and R3 (97 mV). On the other hand, the longer NO_3^- treatment (24 h) caused a significant depolarization (90, 78, 74 mV in R1, R2 and R3, respectively) in all root regions, showing the same pattern among the regions (R1 > R2 > R3) (Fig. 1). Net NO_3^- influx showed a progressive increase (induction phase) which reached a peak of maximum activity (full induction) after 4 h of contact with the anion following by a subsequent decline (decay phase) in all maize root regions (Fig. 2b). Although net NO_3^- influx at the root surface showed a similar trend, it significantly differed among root regions ($p < 0.001$) and at different time of exposure to NO_3^- ($p < 0.001$). In particular, R2 displayed a significant higher NO_3^- influx compared to R1 and R3 at both 0 and 4 h, which disappeared during the decay phase (Fig. 2). On the other hand, net Hþ efflux of R1 was higher at all times of NO_3^- exposure compared to R2 and R3, which in turn showed a similar trend. Notably, the increase of H+ efflux in R1 was already evident after 10 min of NO-3 contact, whereas R2 and R3 showed a similar trend but within 30 min (Fig. 3a). Furthermore, R1 exhibited a marked increase of net H+ flux after 4 h of NO_3^- treatment followed by a decrease at 24 h. This trend was similar to that observed for NO_3^- flux (Fig. 3b). Besides, R2 and R3 showed an increase in net H^+ efflux after 4 h of exposure to NO_3^- but they did not show any reduction (Fig. 3b). Finally, marked differences in $\Delta G/F$ were observed among the root regions ($p < 0.002$) and at different times of exposure to NO_3^- ($p < 0.001$) (Fig. 4). In particular, the R1 region showed higher values of $\Delta G/F$ ratio (Fig. 4).

4.2. Gene expression analysis along maize root

At R1, R2 and R3 regions treated with nitrate the expression patterns of NPF6.3, NRT2.1, NAR2.1, MHA3 and MHA4 over time (0-24 h) were investigated and the results reported in Figs. 5 and 6. The expression of NPF6.3 was not detectable in the root regions or at any NO_3^- exposure time except for R3 region, where a low transcript level could be detected at 0 and 4 h (Fig. 5a). The time course of NRT2.1 expression revealed the presence of transcripts before NO-3 supply (0 h), which markedly increased after 4 h of NO_3^- exposure in all root regions, followed by their decrease at 24 h (Fig. 5b). In particular, the analysis of mRNA abundance of NRT2.1 among root regions showed lower transcript abundance in R1 compared to both R2 and R3 at 0 h. After NO_3^- exposure (4 h), a higher peak of transcripts in R3 compared to R1 and R2 regions was evident. Finally, in the decay phase (at 24 h), no differences in mRNA accumulation among root regions were observed (Fig. 5b). Before exposure to NO_3^-, NAR2.1 showed a similar expression trend in all root regions analyzed. After 4 h, NAR2.1 exhibited the highest transcript levels in R2, which had decreased in all root regions after 24 h of NO_3^- exposure (Fig. 5c). The variation (%) in NRT2.1 and NAR2.1 transcript abundances during the induction (0-4 h of exposure) and decay phases (4-24 h of exposure) was also calculated. In

particular, R1 showed the highest increase in gene expression level (+1100% and +767% in NAR2.1 and NRT2.1, respectively). On the contrary, the R2 root region showed the highest inhibition either for NAR2.1 expression (86%) and NRT2.1 (80%) during the decay phase (Table 1).

The MHA3 amount of transcripts was similar in all root regions, while MHA4 showed a marked peak of transcript accumulation in R2 and R3 at 0 h. Both MHA isoforms increased in the induction phase (4 h): in particular, R1 showed the highest MHA3 transcript level, while R2 exhibited abundance in MHA4 transcript level (Fig. 6a-b). Finally, both MHA isoforms displayed a similar decreasing pattern in all root regions in the decay phase (24 h) (Fig. 6a-b). The highest increase in MHA3 and MHA4 transcript abundances variation (%) was observed in R1 region (+267% MHA3 and +250% in MHA4) during the induction (0-4 h), while R2 showed the highest inhibition in both MHA3 (81%) and MHA4 expressions (86%) during the decay phase (Table 1). Finally, a Pearson correlation between NO_3^- flux and NRT2.1/ NAR2.1 transcript levels during the induction phase in each root region was calculated. The p values of correlation for each individual gene (NRT2.1 and NAR2.1) and NO_3^- flux were not significant. In contrast, there was a strong correlation between NO_3^- flux and the expression both genes NRT2.1 and NAR2 when considered together ($p = 0.00219$) (Table 2).

5. Discussion

Understanding the physiological and molecular mechanisms of root NO_3^- uptake spatial responses to temporal NO_3^- fluctuations in the soil solution is important for agronomical approaches to increase the nitrate uptake efficiency in crops. In the last few decades, high spatial and temporal variability in net nitrate uptake rates along the root axis of several different crop and woody species has been demonstrated, showing the importance of the root tip in nitrate uptake (Colmer and Bloom, 1998; Taylor and Bloom, 1998; Hawkins et al., 2008; Li et al., 2010; Sorgona et al., 2010, 2011; Luo et al., 2013). Previous results demonstrated that maize root regions close to root tip (0-40 mm) exhibited a higher ability to absorb nitrate than the basal ones. However, the transcript abundance of NRT2.1 was temporally, but not spatially correlated with NNUR activity, leading to the hypothesis that NAR2 co-expression needs to cooperate with NRT2.1 to provide NNUR activity along maize root axis (Sorgona et al., 2011). For this reason, we tested this hypothesis by focusing on three maize root regions (R1, R2 and R3) and by applying a noninvasive approaches to analyse NO_3^-/H+ fluxes across the plasma membrane. Consistent with previous results along maize root axis (Sorgona et al., 2011) and in agreement with maize whole-root system data (Hole et al., 1990; Jackson et al., 1973; Locci et al., 2001; Quaggiotti et al., 2003; Santi et al., 2003), all root regions showed different temporal and spatial net fluxes of both ions after NO-3 exposure. In particular, NO_3^- influx was characterized by both induction and decay phases, and this up and down regulation was typical after a starvation period (Glass et al., 2002; Sorgona et al., 2005) and evident in all the root regions. The R1 and R2 regions closer to the root tip appeared more efficient to absorb NO_3^- than the basal one (R3), and the microelectrodes measurement allowed us to evidence that the highest nitrate influx occurred in R2 (about 25 mm from the tip) and was maintained over time. In accordance with these results, a similar temporal level of NRT2.1 and NAR2.1 transcript abundance was observed, showing an increase in their expression during the induction phase followed by a downregulation. The NO-3 influx was not spatially correlated with each single NRT2.1 or NAR2.1 gene expression along the root axis. However, when NAR2.1 and NRT2.1 transcripts were considered together, a highly significant correlation with NO-3 influxes was observed ($p = 0.0023$) (Table 2). These results supported our initial hypothesis, indirectly demonstrating for the first time the functional interaction between NRT2.1 transporter and a NAR-like partner for nitrate uptake along maize root axis, as already

reported in Chlamydomonas reinhardtii (Zhou et al., 2000), Hordeum vulgare (Tong et al., 2005), Oryza sativa (Yan et al., 2011) and Arabidopsis thaliana (Okamoto et al., 2006; Yong et al., 2010).

In accordance with the role of NRT2.1 transporter operating for iHATS, the root regions exposed to 50 μM external NO_3^- and characterized by high NNUR showed a higher expression of NRT2 compared to the low affinity NPF6.3 transporter which operated for LATS (>500 mM external NO-3). As a consequence, R1 and R2 did not show any NPF6.3 expression, which was detectably expressed only in R3. The spatial and temporal profiles of net H+ efflux along maize roots were significantly different. Notably, net H+ efflux was temporally, but not spatially correlated with NO-3 influx, increasing during the induction phase of NO_3^- uptake and declining in the decay phase in all the root regions. In accordance with Hawkins et al. (2008), R1 showed higher net H+ efflux compared to the other regions over time, while no significant difference between R2 and R3 was observed. Increased H+ efflux was correlated with an enhanced temporal expression of both MHA3 and MHA4, similar to that observed in NO_3^- uptake, confirming the critical role played by PM H+-ATPase in NO-3 uptake along maize root (Sorgona et al., 2011). However, after 4 h of NO_3^- exposure (induction phase), MHA3 showed the highest expression in R1, while MHA4 transcript abundance was higher in R2. These results confirmed the different role of these PM H+-ATPase isoforms in roots, as already reported (Santi et al., 1995; Quaggiotti et al., 2003), and MHA4 appeared more sensitive to nitrate with a distinct up- and down-regulation than MHA3 (Santi et al., 2003), suggesting a different role played by R1 and R2, characterized by greatest proton and NO_3^- fluxes, respectively. Since membrane potential can be considered as an indicator of the cell energy status depending on intra-and extracellular features (Sze et al., 1999; Miller et al., 2001), the spatialtemporal variation of this parameter along root axis and over time, was analyzed. Regardless of nitrate treatment, R1 showed a relatively greater membrane hyperpolarization compared to R2 and R3, in accordance with the observed H+ efflux pattern depending on PM H+-ATPase activity (McClure et al., 1990). This change in membrane potential was maintained after the nitrate treatment (4 and 24 h). Furthermore, the higher extrusion and the lower surface pH in R1 compared to R2 and R3 may stimulate cell wall expansion and/or establish a greater electrochemical gradient to drive solute uptake, and maintain turgor in the expansion zone during nitrate treatments (Bloom et al., 2003). This assumption was also confirmed by thermodynamic and free energy status, where R1 showed the higher values compared to R2 and R3, at all times of nitrate exposure, highlighting possibly higher metabolic activity, enhanced uptake and sensitivity nearer the root apex. Overall, our results demonstrated for the first time the functional interaction between NRT2.1 transporter and NAR2 accessory protein for nitrate acquisition along the maize root axis. The H+ efflux and NO-3 influx together with NRT2.1/NAR2.1 and MHA3/ MHA4 expression patterns, suggest different roles played by the R1 and R2 regions in response to nitrate. The first root region (R1) appeared to be more sensitive to nutritional and metabolic external stimuli, while R2 was mainly involved in nitrate acquisition. Recently, Trevisan et al. (2015) showed that the Transition Zone (TZ) in primary maize root, corresponding to our R1 region, is the critical zone for sensing nitrate and/or environmental stimuli, whereas R2 may be considered as the root zone assigned to uptake nitrate. Together these different methodological approaches for studying nitrate fluxes along maize roots seem to have arrived at similar conclusions.

6. Contribution

A.L., F.M., F.S. and M.R.A. conceived, designed the experiments, analyzed the data. A.L, F.M., and F.A. performed the experiments. AJM revised advised on the preparation of the manuscript. A.L., F.S., M.R.A. wrote the manuscript.

References

Barbier-Brygoo, H., De Angeli, A., Filleur, S., Frachisse, J.M., Gambale, F., Thomine, S., Wege, S., 2011. Anion channels/transporters in plants: from molecular bases to regulatory networks. Annu. Rev. Plant Biol 62, 25e51. http://dx.doi.org/10.1146/ annurev-arplant-042110-103741.

Bloom, A.J., Meyerhoff, P.A., Taylor, A.R., Rost, T.L., 2003. Root development and absorption of ammonium and nitrate from the rizosphere. J. Plant Growth Regul. 21, 416e431. http://dx.doi.org/10.1007/s00344-003-0009-8.

Colmer, T.D., Bloom, A.J., 1998. A comparison of NHþ4 and NO3 net fluxes along roots of rice and maize. Plant Cell Environ. 21, 240e246. http://dx.doi.org/10.1046/j. 1365-3040.1998.00261.x.

Crawford, N.M., Glass, A.D.M., 1998. Molecular and physiological aspects of nitrate uptake in plants. Trends Plant Sci. 3, 389e395. http://dx.doi.org/10.1016/S13601385(98)01311-9.

El-kereamy, A., Guevara, D., Bi, Y.-M., Chen, X., Rothstein, S.J., 2011. Exploring the molecular and metabolic factors contributing to the adaptation of maize seedlings to nitrate limitation. Front. Plant Sci. 2 Artic. 49, 1e15. http://dx.doi. org/10.3389/fpls.2011.00049.

Garnet, T., Conn, V., Plett, D., Conn, S., Zanghellini, J., Mackenzie, N., Enju, A., Francis, K., Holtham, L., Roessner, U., Boughton, B., Bacic, A., Shirley, N., Rafalski, A., Dhugga, K., Tester, M., Kaiser, B.N., 2013. The response of the maize nitrate transport system to nitrogen demand and supply across the lifecycle. New Phytol. 198, 82e94. http://dx.doi.org/10.1111/nph.12166.

Glass, A.D., Britto, D.T., Kaiser, B.N., Kinghorn, J.R., Kronzucker, H.J., Kumar, A., Okamoto, M., Rawat, S., Siddiqi, M.Y., Unkles, S.E., Vidmar, J.J., 2002. The regulation of nitrate and ammonium transport systems in plants. J. Exp. Bot. 53, 855e864. http://dx.doi.org/10.1093/jexbot/53.370.855.

Glass, A.D.M., 2009. Nitrate uptake by plant roots. Botany 87, 659e667. http://dx. doi.org/10.1139/B09-014.

FAO, 2006. Fertilizer Use by Crop. FAO Fertilizer and Plant Nutrition Bulletin, Rome.

Hawkins, B.J., Boukcim, H., Plassard, C., 2008. A comparison of ammonium, nitrate and proton net fluxes along seedling roots of Douglas-fir and lodgepole pine grown and measured with different inorganic nitrogen sources. Plant Cell Environ. 31, 278e287. http://dx.doi.org/10.1111/j.1365-3040.2007.01760.x.

Henriksen, G.H., Raj Raman, D., Walker, L.P., Spanswick, R.M., 1992. Measurement of net fluxes of ammonium and nitrate at the surface of barley roots using ionselective microelectrodes II. Patterns of uptake along the root axis and evaluation of the microelectrode flux estimation technique. Plant Physiol. 99, 734e747. http://dx.doi.org/10.1104/pp.99.2.734.

Ho, C.H., Lin, S.H., Hu, H.C., Tsay, Y.F., 2009. CHL1 functions as a nitrate sensor in plants. Cell 138, 1184e1194. http://dx.doi.org/10.1016/j.cell.2009.07.004.

Hole, J.D., Emra, A.M., Fares, Y., Drew, M.C., 1990. Induction of nitrate transport in maize roots, and kinetics of influx, measured with nitrogen-13. Plant Physiol. 93, 642e647. http://dx.doi.org/10.1104/pp.93.2.642.

Jackson, W.A., Flesher, D., Hageman, R.H., 1973. Nitrate uptake by dark grown corn seedlings. Some characteristics of apparent induction. Plant Physiol. 51, 120e127. http://dx.doi.org/10.1104/pp.51.1.120.

Krouk, G., Lacombe, B., Bielach, A., Perrine-Walker, F., Malinska, K., Mounier, E., Hoyerova, K., Tillard, P., Leon, S., Ljung, K., Zazimalova, E., Benkova, E., Nacry, P., Gojon, A., 2010. Nitrate-regulated auxin transport by NRT1.1 defines a mechanism for nutrient sensing in plants. Dev. Cell 18, 927e937. http://dx.doi.org/10. 1016/j.devcel.2010.05.008.

Leran, S., Varala, K., Boyer, J.-C., Chiurazzi, M., Crawford, N., Daniel-Vedele, F., David, L., Dickstein, R., Fernandez, E., Forde, B., Gassmann, W., Geiger, D., Gojon, A., Gong, J.M., Halkier, B.A., Harris, J.M., Hedrich, R., Limami, A.M., Rentsch, D., Seo, M., Zhang, M., Coruzzi, G., Lacombe, B., 2014. A unified nomenclature of nitrate transporter 1/peptide transporter family members in plants. Trends Plant Sci. 19, 5e9. http://dx.doi.org/10.1016/j.tplants.2013.08.008.

Li, Q., Li, B.H., Kronzucker, H.J., Shi, W.M., 2010. Root growth inhibition by NHþ4 in Arabidopsis is mediated by the root tip and is linked to NHþ4 efflux and GMPase activity. Plant Cell Environ. 33, 1529e1542. http://dx.doi.org/10.1111/j.13653040.2010.02162.x.

Li, W., Wang, Y., Okamoto, M., Crawford, N.M., Siddiqi, M.Y., Glass, A.D.M., 2007. Dissection of the AtNRT2.1, AtNRT2.2 inducible high-affinity nitrate transporter gene cluster. Plant Physiol 143, 425e433. http://dx.doi.org/10.1104/pp.106. 091223.

Livak, K.J., Schmittgen, T.D., 2001. Analysis of relative gene expression data using real-time quantitative PCR and the 2-DDCT method. Methods 25, 402e408. http://dx.doi.org/10.1006/meth.2001.1262.

Locci, G., Santi, S., Monte, R., Pinton, R., Varanini, Z., 2001. Involvement of plasma membrane Hþ-ATPase in nitrate uptake by maize genotypes. In: Horst, W.J., Shenk, M.K., Bürker, A., Claassen, N., Flessa, H., Frommer, W.B., Goldbach, H., Olfs, H.-W., Ro€mheld, V., Settelmacher, B., Schmidhalter, U., Schubert, S., von Wiren, N., Wittenmayer, L. (Eds.), Plant Nutrition e Food Security and Sustainability of Agro-ecosystems. Kluwer Academic Publishers, Dordrecht, The Netherlands, pp. 184e185.

Luo, J., Qin, J., He, F., Li, H., Liu, T., Polle, A., Peng, C., Luo, Z.-B., 2013. Net fluxes of ammonium and nitrate in association with Hþfluxes in fine roots of Populus popularis. Planta 237, 919e931. http://dx.doi.org/10.1007/s00425-012-1807-7.

Lupini, A., Sorgona, A., Miller, A.J., Abenavoli, M.R., 2010. Short-time effects of coumarin along the maize primary root axis. Plant Signal. Behav. 5, 1395e1400. http://dx.doi.org/10.4161/psb.5.11.13021.

Masclaux-Daubresse, C., Daniel-Vedele, F., Dechorgnat, J., Chardon, F., Gaufichon, L., Suzuki, A., 2010. Nitrogen uptake, assimilation and remobilitation in plants: challenges for sustainable and productive agriculture. Ann. Bot. 105, 1141e1157. http://dx.doi.org/10.1093/aob/mcq028.

McClure, P.R., Koc, L.V., Spanswick, R.M., Shaff, J.E., 1990. Evidence for cotransport of nitrate and protons in maize roots 1. Effects of nitrate on the membrane potential. Plant Physiol. 93, 281e289. http://dx.doi.org/10.1104/pp.93.1.281.

Miller, A.J., Cookson, S.J., Smith, S.J., Wells, D.M., 2001. The use of microelectrodes to investigate compartmentation and the transport of metabolized inorganic ions in plants. J. Exp. Bot. 52, 541e549. http://dx.doi.org/10.1093/jexbot/52.356.541.

Miller, A.J., Fan, X., Orsel, M., Smith, S.J., Wells, D., 2007. Nitrate transport and signaling. J. Exp. Bot. 58, 2297e2306. http://dx.doi.org/10.1093/jxb/erm066.

Miller, A.J., Smith, S.J., 1996. Nitrate transport and compartmentation in cereal root cells. J. Exp. Bot. 300, 843e854. http://dx.doi.org/10.1093/jxb/47.7.843.

Nacry, P., Bouguyon, E., Gojon, A., 2013. Nitrogen acquisition by roots: physiological and developmental mechanisms ensuring plant adaptation to a fluctuating resource. Plant Soil 370, 1e27. http://dx.doi.org/10.1007/s11104-013-1645-9.

Newman, I.A., 2001. Ion transport in roots: measurement of fluxes using ionselective microelectrodes to characterize transporter function. Plant Cell Environ. 24, 1e14. http://dx.doi.org/10.1046/j.1365-3040.2001.00661.x.

Okamoto, M., Kumar, A., Li, W., Wang, Y., Siddiqi, M.Y., Crawford, N.M., Glass, A.D.M., 2006. High-affinity nitrate transport in roots of Arabidopsis depends on expression of the NAR2-like gene AtNRT3.1. Plant Physiol. 140, 1036e1046. http://dx.doi.org/10.1104/pp.105.074385.

Okamoto, M., Vidmar, J.J., Glass, A.D., 2003. Regulation of NRT1 and NRT2 gene families of Arabidopsis thaliana: responses to nitrate provision. Plant Cell Physiol 44, 304e317. http://dx.doi.org/10.1093/pcp/pcg036.

Orsel, M., Chopin, F., Leleu, O., Smith, S.J., Krapp, A., Daniel-Vedele, F., Miller, A.J., 2006. Characterization of a two-component high-affinity nitrate uptake system in Arabidopsis. Physiology and protein-protein interaction. Plant Physiol. 142, 1304e1317. http://dx.doi.org/10.1104/pp.106.085209.

Quaggiotti, S., Ruperti, B., Borsa, P., Destro, T., Malagoli, M., 2003. Expression of a putative high-affinity NO-3 transporter and of an Hþ-ATPase in relation to whole plant nitrate transport physiology in two maize genotypes differently responsive to low nitrogen availability. J. Exp. Bot. 54, 1023e1031. http://dx.doi.org/10.

1093/jxb/erg106.

Santi, S., Locci, G., Monte, R., Pinton, R., Varanini, Z., 2003. Induction of nitrate uptake in maize roots: expression of a putative high-affinity nitrate transporter and plasma membrane Hþ-ATPase isoforms. J. Exp. Bot. 54, 1851e1864. http:// dx.doi.org/10.1093/jxb/erg208.

Santi, S., Locci, G., Pinton, R., Cesco, S., Varanini, Z., 1995. Plasma membrane HþATPase in maize roots induced for NO-3 uptake. Plant Physiol. 109, 1277e1283. http://dx.doi.org/10.1104/pp.109.4.1277.

Sorgona, A., Abenavoli, M.R., Cacco, G., 2005. A comparative study between two Citrus rootstocks: effect of nitrate on the root morpho-topology and net nitrate uptake. Plant Soil 270, 257e267. http://dx.doi.org/10.1007/s11104-004-1607-3.

Sorgona, A., Cacco, G., Di Dio, L., Schmidt, W., Perry, P.G., Abenavoli, M.R., 2010. Spatial and temporal patterns of net nitrate uptake regulation and kinetics along the tap root of Citrus aurantium. Acta Physiol. Plant. 32, 683e693. http:// dx.doi.org/10.1007/s11738-009-0447-4.

Sorgona, A., Lupini, A., Mercati, F., Di Dio, L., Sunseri, F., Abenavoli, M.R., 2011. Nitrate uptake along the maize primary root: an integrated physiological and molecular approach. Plant Cell Environ. 34, 1127e1140. http://dx.doi.org/10.1111/j. 1365-3040.2011.02311.x.

Sze, H., Li, X.H., Palmgren, M.G., 1999. Energization of plant cell membranes by Hþpumping ATPases: regulation and biosynthesis. Plant Cell 11, 677e689. http:// dx.doi.org/10.1105/tpc.11.4.677.

Taylor, A.R., Bloom, A.J., 1998. Ammonium, nitrate, and proton fluxes along the maize root. Plant Cell Environ. 21, 1255e1263. http://dx.doi.org/10.1046/j.13653040.1998.00357.x.

Tong, Y., Zhou, J.J., Li, Z., Miller, A.J., 2005. A two-component high-affinity nitrate uptake system in barley. Plant J. 41, 442e450. http://dx.doi.org/10.1111/j.1365313X.2004.02310.x.

Trevisan, S., Manoli, A., Ravazzolo, L., Botton, A., Pivato, M., Masi, A., Quaggiotti, S., 2015. Nitrate sensing by the maize root apex transition zone: a merged transcriptomic and proteomic survey. J. Exp. Bot. 66, 3699e3715. http://dx.doi.org/ 10.1093/jxb/erv165.

Wirth, J., Chopin, F., Santoni, V., Viennois, G., Tillard, P., Krapp, A., Lejay, L., DanielVedele, F., Gojon, A., 2007. Regulation of root nitrate uptake at the NRT2.1 protein level in Arabidopsis thaliana. J. Biol. Chem. 282, 23541e23552. http://dx. doi.org/10.1074/jbc.M700901200.

Yan, M., Fan, X., Feng, H., Miller, A.J., Shen, Q., Xu, G., 2011. Rice OsNAR2.1 interacts with OsNRT2.1, OsNRT2.2 and OsNRT2.3a nitrate transporters to provide uptake over high and low concentration ranges. Plant Cell Environ. 34, 1360e1372. http://dx.doi.org/10.1111/j.1365-3040.2011.02335.x.

Yong, Z., Kotur, Z., Glass, A.D., 2010. Characterization of an intact two-component high-affinity nitrate transporter from Arabidopsis roots. Plant J. 63, 739e748. http://dx.doi.org/10.1111/j.1365-313X.2010.04278.x.

Zamboni, A., Astolfi, S., Zuchi, S., Pii, Y., Guardini, K., Tononi, P., Varanini, Z., 2014. Nitrate induction triggers different transcriptional changes in a high and low nitrogen use efficiency maize inbred line. J. Integr. Plant Biol. 56, 1080e1094. http://dx.doi.org/10.1111/jipb.12214.

Zhou, J.J., Fernandez, E., Galvan, A., Miller, A.J., 2000. A high affinity nitrate transport system from Chlamydomonas requires two gene products,. FEBS Lett 466, 225e227.

Table 1.Percentage variation in the ZmNAR2.1, ZmNRT2.1, MAH3 and MAH4 transcript levels observed during the induction (% increase from 0 to 4 h) and decay phases (% decrease from 4 to 24 h).

	Induction phase			Decay phase		
	R1	R2	R3	R1	R2	R3
NAR2.1	1100	350	400	71	86	73
NRT2.1	767	233	611	54	80	78
MHA3	267	125	100	64	81	83
MHA4	250	79	64	66	86	73

Table 2. Pearson correlation between nitrate flux and transcript level of ZmNRT2.1, ZmNAR2.1 independently and in combination (NRT2.1 plus NAR2.1) during the induction phase in maize primary root.

Transcipt	Linear equation	R2	P
NRT2.1	Y = 0.1752X+16.246	0.876	0.064^{NS}
NAR2.1	Y = 0.1155X+39.08	0.888	0.0573^{NS}
NRT2.1 plus NAR2.1	Y = 0.0784X+19.842	0.995	0.00219*

NS = no significant; * = significant at $p < 0.05$.

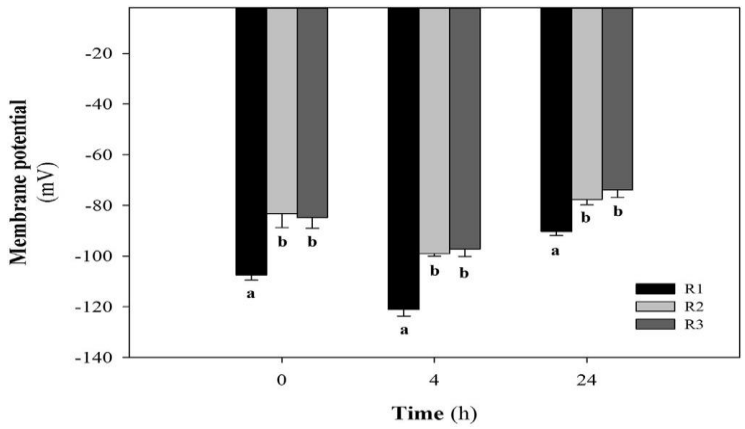

Fig. 1. Cell membrane potential in R1, R2 and R3 regions of primary maize root after 0, 4 and 24 h of exposure to 50 mM KNO3. The values are presented as mean ± SE (n ¼ 5). Different letters within the time indicate means that differ significantly, according to Tukey's HSD test at $p < 0.05$.

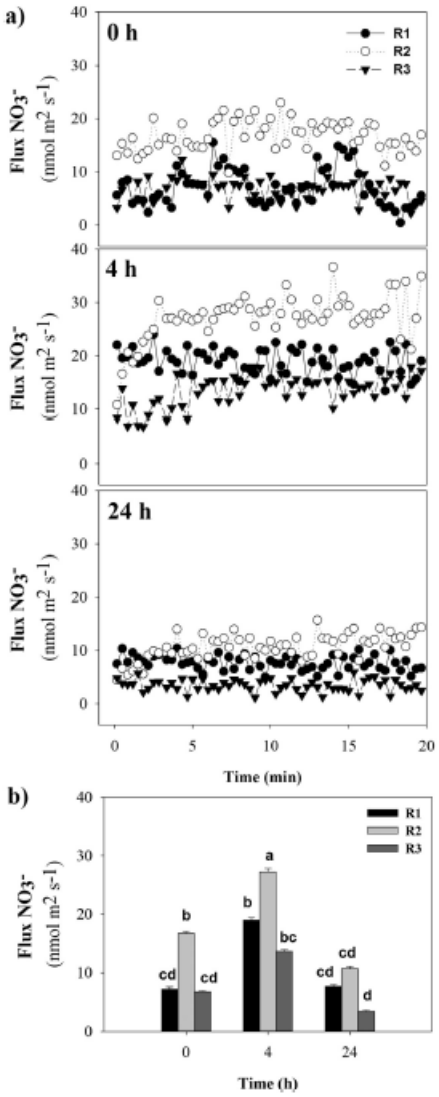

Fig. 2. NO3 - fluxes in response to 0, 4 and 24 h of exposure to 50 mM nitrate (a), and mean flux within the measuring period (b). Measurements were made in the primary root at 10, 30 and 50 mm from the root tip. The values are presented as mean ± SE (n ¼ 5). Different letters indicate means that differ significantly, according to Tukey's HSD test at $p < 0.05$.

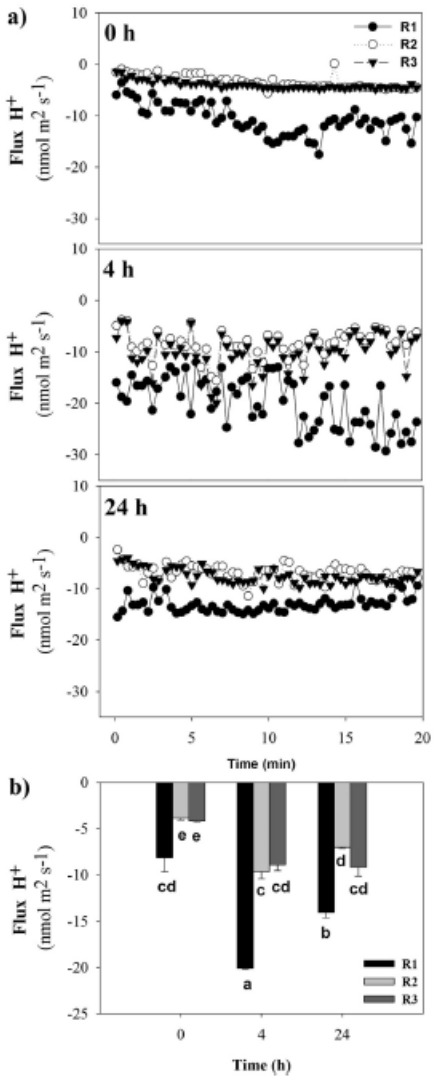

Fig. 3. H+ fluxes in response to 0, 4 and 24 h of exposure to 50 mM nitrate (a), and mean flux within the measuring period (b). Measurements were made in the primary root at 10, 30 and 50 mm from the root tip. The values are presented as mean ± SE (n=5). Different letters indicate means that differ significantly, according to Tukey's HSD test at $p < 0.05$.

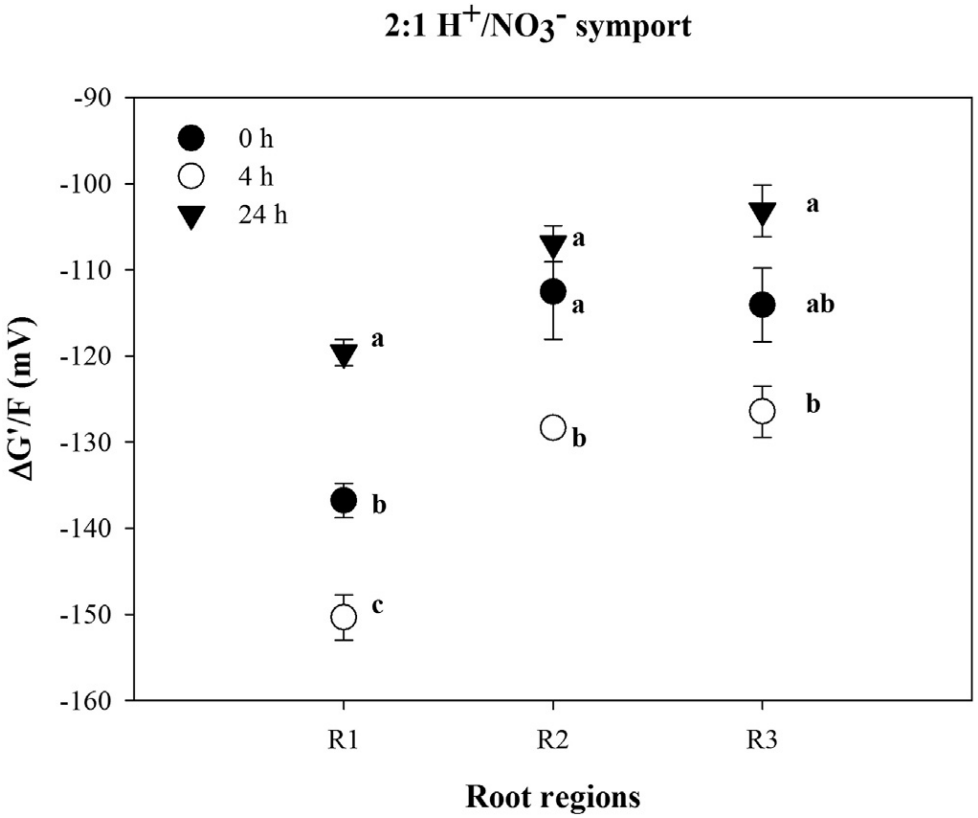

Fig. 4. Calculation of DG/F for a plasma membrane symport mechanism with 2:1Hþ:NO3 - stoichiometry along the maize root axis. The values are presented as mean ± SE (n= 5). Different letters within the region indicate means that differ significantly, according to Tukey's HSD test at $p < 0.05$.

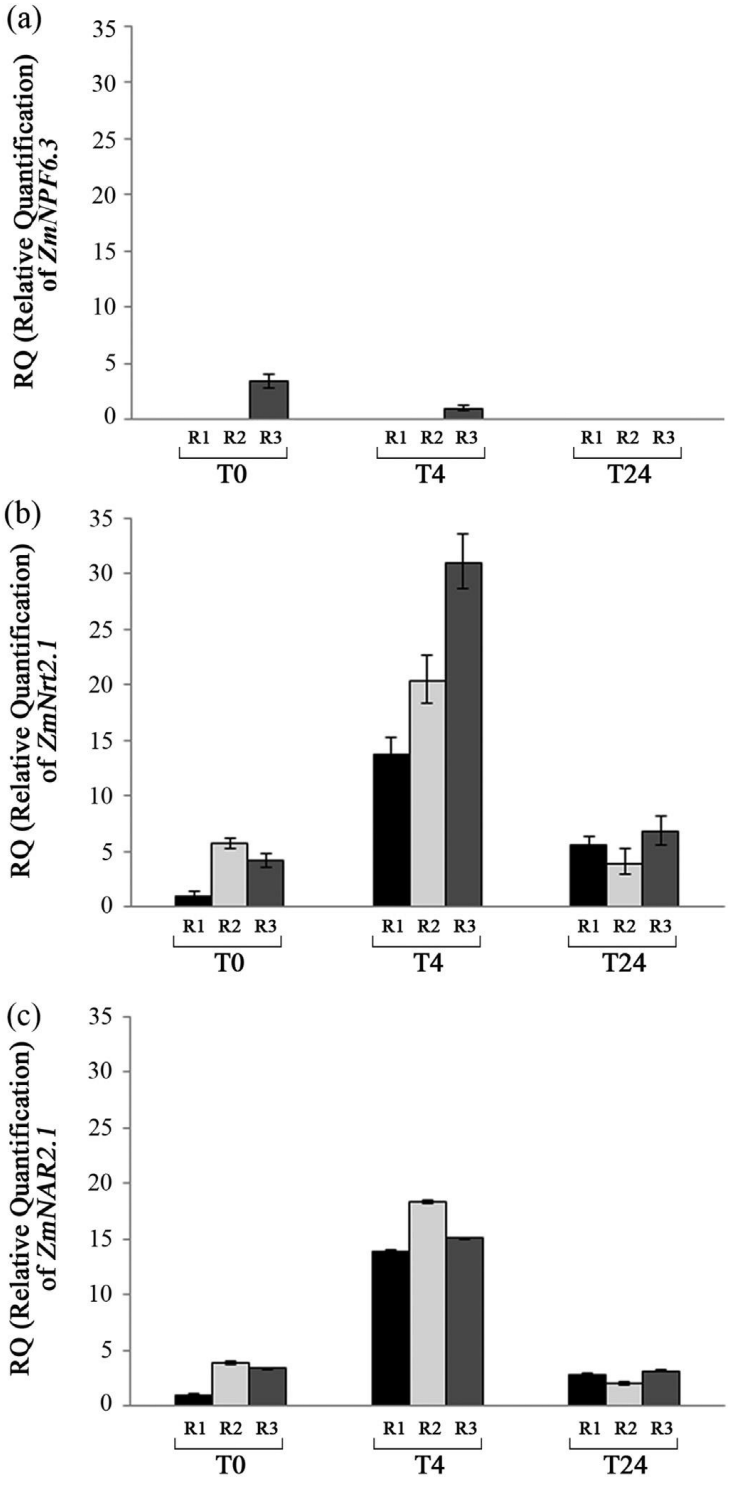

Fig. 5. Gene expression analysis of ZmNPF6.3, ZmNRT2.1 and ZmNAR2.1 in different root regions (R1, R2 and R3) of maize seedlings exposed to 50 mMNO3 - for 0 (T0), 4 (T4) and 24 (T24) hours. (a), (b), and (c): quantification of ZmNPF6.3, ZmNRT2.1 and ZmNAR2.1 transcript accumulation in root regions was evaluated by qPCR. Ubiquitin was used as a reference housekeeping gene. The relative quantification of gene transcript level was performed using $2^{-\Delta\Delta CT}$ comparative method as described in Materials and Methods.

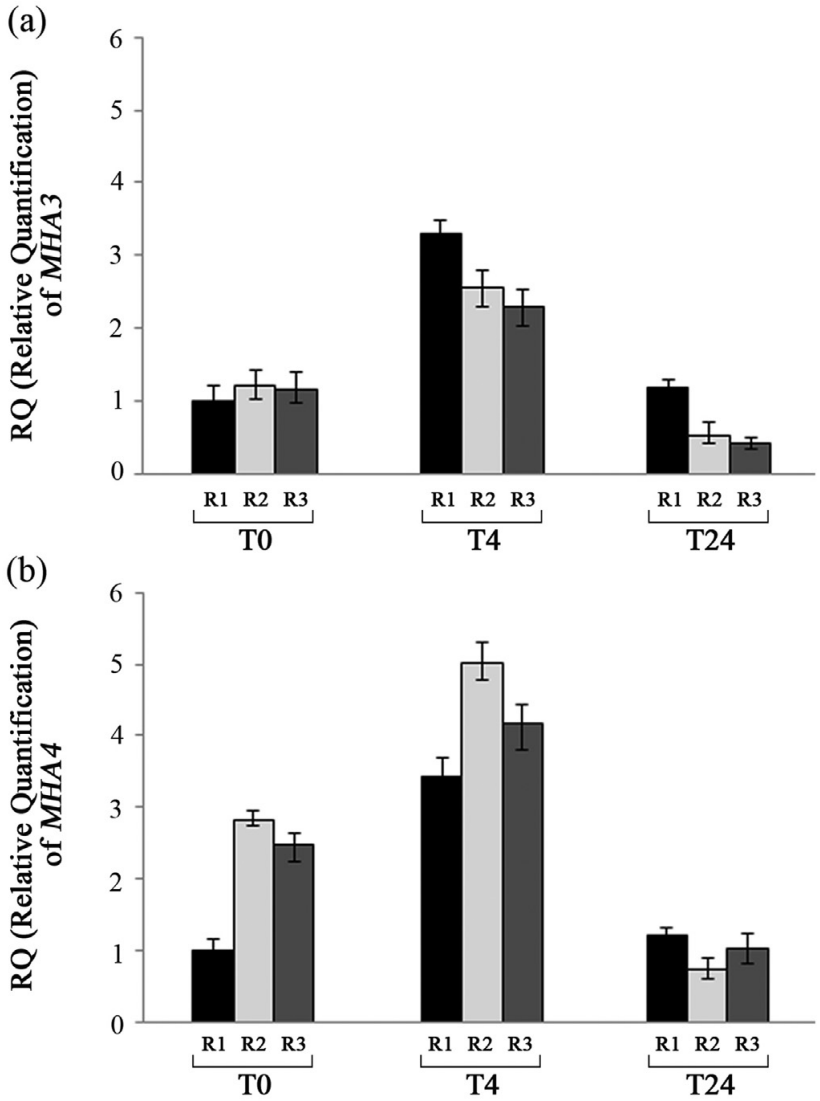

Fig. 6. Gene expression analysis MHA3 and MHA4 in different root regions (R1, R2 and R3) of maize seedlings exposed to 50 mMNO3 - for 0 (T0), 4 (T4) and 24 (T24) hours. (a), (b): quantification of MHA3 and MHA4 transcript accumulation in root regions was evaluated by qPCR. Ubiquitin was used as a reference housekeeping gene. The relative quantification of gene transcript level was performed using 2-DDCT comparative method as described in Materials and Methods.